Insights into the Thermodynamics of Hydricity for a Rhenium Pincer Complex and their Implications on Catalytic Conditions

By
Jenny Hu

Senior Honors Thesis
Department of Chemistry
University of North Carolina at Chapel Hill

April 22, 2020

Approved:

_____

Alexander Miller, Thesis Advisor
John Papanikolas, Reader
Aleksandr Zhukhovitskiy, Reader

Abstract:
Thermodynamic considerations regarding critical hydrogenation reactions have not been well studied. We report a rhenium(I) pincer carbonyl complexes have been synthesized. Hydricity values, as well as the enthalpy and entropy of H_2 heterolysis, have been experimentally determined in various solvents (THF, MeCN, toluene). Preliminary catalytic hydrogenation reactions of CO_2 have been carried out using (^{tBu}POCOP)(Re)(CO)$_2$(H)$^-$.

Introduction:
The formation of methanol as long been an essential reaction underpinning global industries including pharmaceutical, agricultural, and cosmetic processes.[1,2] Current industrial methanol synthesis relies on hydrogenation of CO, which is formed from fossil fuels (Figure 1A).[3] These processes are not only energy intensive, but are not carbon-neutral. As a result, greener approaches are necessary to reduce the carbon-footprint of this industrial process. One such effort is through multi-step hydrogenation of CO_2 via esterification/amidification of formic acid intermediates (Figure 1B).[1,2,4] This CO_2-derived process would achieve a carbon-neutral cycle.

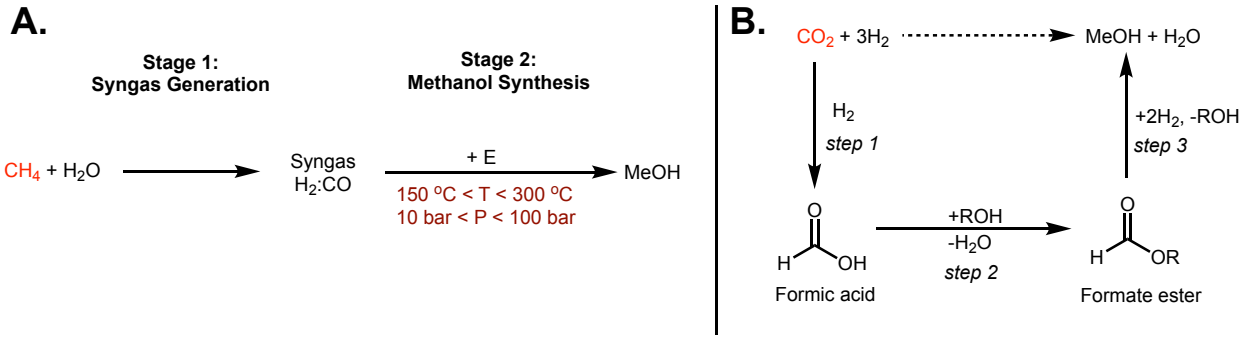

Figure 1: (A) Current industrial methods for synthesis of methanol.[3] (B) General catalytic scheme of CO_2 hydrogenation using H_2.

Unfortunately, hydrogenation of the intermediate esters or amides is significantly harder than CO_2 due to higher thermodynamic barriers and unwanted side reactions.[2] Historically, these reactions have been driven by stoichiometric amounts of metal hydrides (e.g. $LiAlH_4$, $NaBH_4$).[1] These reactions not only create substantial waste, but are also not economically plausible. More recently, homogeneous transition metal catalysts have been shown to drive these reactions with high yields and selectivity. However, they typically require high pressures (often at 50 bar H_2) and temperatures (in excess of 100 ºC).[1,2]

If we can better understand the thermodynamics of individual steps of metal hydride catalysis, it may be possible to design systems able to perform these reactions at milder conditions, with greater selectivity and catalyst activity. One important reaction step in transition metal hydrogenation catalysis is in the transfer of H^- from metal to substrate. Governed by the thermodynamic parameter of hydricity, ΔG^o_{H-}, stronger hydride donors have lower ΔG^o_{H-} values. Transfer of the

H^- ion should be more favorable from an anionic transition metal hydride and provide greater thermodynamic driving force for hydride transfer to less electrophilic carboxylate derivatives.[6,7]

Hydricity can be determined using the equations described in **Scheme 1.** The K_{eq} value in **Eq. 1** is experimentally determined by allowing equilibration between metal and metal hydride in solution with base under an atmosphere of hydrogen. pK_a and H_2 heterolysis values are reported in the literature. The results of **Eq. 1–3** are summed to yield hydricity.

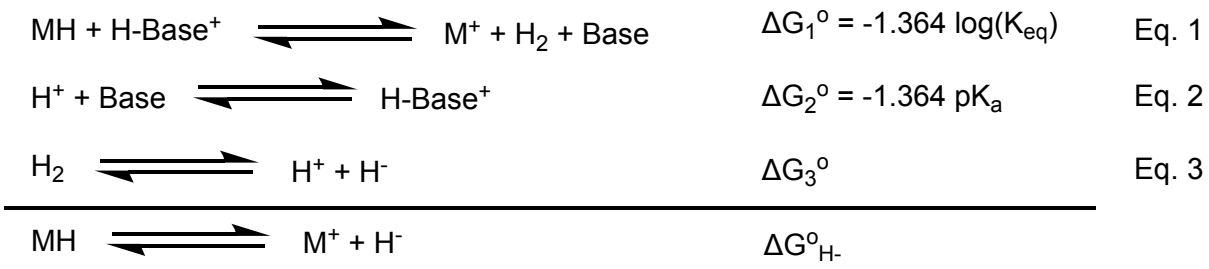

Scheme 1: *Determination of hydricity through heterolysis of H_2.*[6]

Hydricity measurements in organic solvents such as THF or toluene face challenges because, until recently, the H_2 heterolysis (ΔG_3^o) constant was not known.[7] Additionally, because the equations in **Scheme 1** rely on equilibrium constants involving gases, the hydricity should be both pressure and temperature-dependent, though these effects have remained unexplored. Intuitively, at the increased pressures utilized in catalysis, the K_{eq} in **Eq. 1** should shift to favor hydride formation, as higher pressures should lead to increased H_2 solubility, driving the reaction towards the left. Similar arguments can be made for decreasing the temperature of reaction, which increases the solubility of hydrogen gas into solution and reduces entropic penalties. This leads to increased production of metal hydride.

With these values in hand, it would be possible to determine the favorability of hydrogenation reactions such as the transfer of a hydride from the metal catalyst to CO_2. In addition, direct comparisons of reaction rates in different solvents could be obtained.

To understand the fundamental thermodynamics of these homogeneous catalysts, a metal hydride complex exhibiting easily measurable K_{eq} (**Eq. 1**) under various conditions that is sufficiently hydridic to perform these hydrogenation reactions is required. Previous reports on rhenium pincer complexes show promising reactivity towards CO_2 and its derivatives, which acted as starting point for our studies.[8,9] Building off this work, we noted that early metal hydrides were typically more hydridic, and, by modifying the ligand structure, we could access an anionic metal hydride that should also increase hydricity.

Herein we report $[(^{tBu}POCOP)Re(H)(CO)_2]^-$, an anionic rhenium hydride that is sufficiently hydridic to reduce CO_2 in a variety of solvents while also exhibiting solvent and temperature-

dependent H_2 heterolysis equilibria. This is the first reported hydricity values for a rhenium hydride complex. Initial applications of these principles have also been explored.

Results and Discussion:

Synthesis of rhenium carbonyl complexes

New rhenium(I) complexes with anionic pincer ligands were sought. Refluxing ^{tBu}POCOP (^{tBu}POCOP = 2,6-bis(di-*tert*-butyl phosphonito)benzene) with $Re(CO)_5Cl$ and triethylamine in chlorobenzene for 16 h led to formation of a colorless solid. Upon recrystallization from cold pentane, **1** could be isolated in >99% purity (by ^{1}H NMR). The appearance of a "virtual triplet" tert-butyl resonances in the 1H NMR spectrum, due to phosphorus coupling through the metal center, led us to conclude that metalation was successful. In addition, the appearance of a single *tert*-butyl resonance revealed a symmetric molecule above and below the pincer ligand plane, allowing us to assign the species as (^{tBu}POCOP)$Re(CO)_3$ **(1)**. CO stretching frequencies can be observed through IR spectroscopy at 1902 cm^{-1}, 1923 cm^{-1}, and 2023 cm^{-1}, which is expected for a meridional geometry. Other similar rhenium(I) carbonyls report stretching frequencies in the same area.[10,11] This assignment was confirmed through single-crystal X-ray diffraction of crystals grown from a cold pentane solution (**Figure 2**). **1** was determined to be octahedral in geometry, with Re–P bond lengths of 2.4354 Å and 2.4195 Å, Re–C bond lengths 1.958 Å (C1), 1.941 Å (C2), 1.994 Å (C3) and 2.176 Å (C4), and C–O bond lengths, 1.151 Å (C1–O1), 1.161 Å (C2–O2), and 1.150 Å (C3–O3).

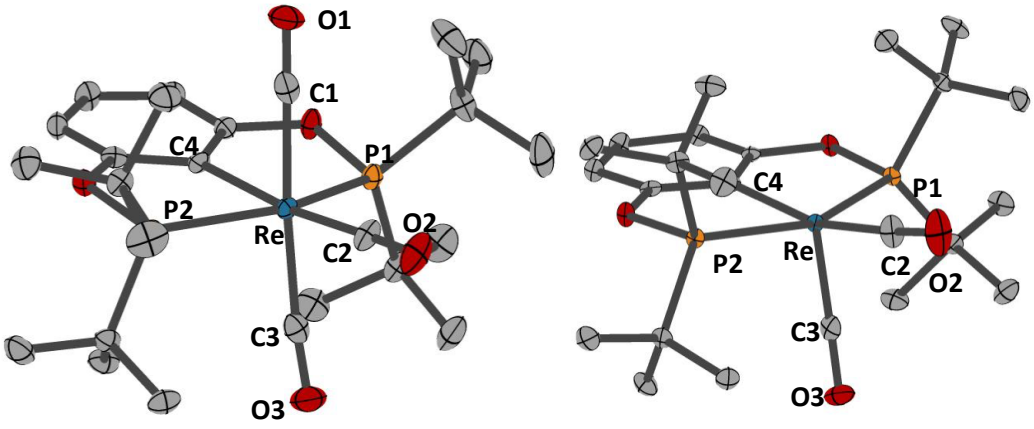

Figure 2: *Crystal structure of* (^{tBu}POCOP)$Re(CO)_3$ **(1)** *(left) and* (^{tBu}POCOP)$Re(CO)_2$ (**2**) *(right).*

With **1** in hand, we looked to open a coordination site for H_2 activation and hydride formation. Decarbonylation attempts included photolysis (405 nm) and oxygen atom transfer (Me_3NO, Lut-NO, iodosobenzene) led to decomposition, while thermolysis (200 °C) afforded only partial conversion to a new species. Though traditional decarbonylation methods proved unsuccessful, thermolysis of **1** with excess lithium triethylborohydride ($LiHBEt_3$, 1M in THF) at 70 °C in THF

led to CO replacement with a hydride ligand (**Figure 3**). Subsequent removal of any liberated CO via a freeze-pump-thaw cycle and addition of HCl led to vigorous H_2 evolution and an instant color change to dark brown. ^1H and $^{31}P\{^1H\}$ NMR spectroscopy of the brown solid showed a 30 ppm shift of the phosphorus resonance (δ 210), along with shifts of the *tert*-butyl and aromatic proton resonances. X-ray diffraction of single crystals grown from a cold pentane solution led to the definitive assignment of the structure as (^{tBu}POCOP)Re(CO)$_2$ (**2**) (**Figure 2**). Re–P bond lengths in **1** and **2** are essentially the same (2.3814 Å and 2.3789 Å respectively) while the Re–C3 bond lengths in axial CO ligands contracts from 1.994 Å in **1** to 1.838 Å in **2**, likely due to increased orbital interaction with the metal center and the lack of competition from a *trans* CO ligand. The contraction of the Re–C3 bond is concomitant with slight lengthening of the C3–O3 bond by 0.02 Å. Two carbonyl stretches were observed by IR at 1834 and 1911 cm^{-1}. Due to decreased competition for electrons at the metal center, the CO ligands in **2** are bound tighter through back-bonding and thus much more activated than in **1**.

After clean synthesis of **2** was achieved, the synthesis of [(^{tBu}POCOP)ReH(CO)$_2$]$^-$ (**3**) was targeted. Addition of NaHBEt$_3$ (1M in toluene) to **2** at room temperature in toluene led to no initial reaction. Upon addition of excess pentane, the solution slowly lightened in color as a white precipitate formed. After 16 h, the solution was decanted, briefly dried, and ^1H and $^{31}P\{^1H\}$ NMR spectra were acquired in freshly dried THF-d_8. A triplet at -6.33 ppm in the ^1H NMR spectroscopy implied the formation of a metal hydride. In addition, symmetry was broken in the compound, as reflected in two distinct *tert*-butyl resonances (δ 1.33 and 1.44). An IR spectrum taken in THF-d_8 revealed two new peaks at 1873 cm^{-1} and 1754 cm^{-1}, signifying further activation of the carbonyl ligands. A shoulder on the 1754 cm^{-1} may be also suggestive of a hydride stretch. Efforts to further dry **3** proved untenable, as the solid was unstable to vacuum, slowly turning from white to a dark orange-brown. Subsequent dissolution of the colored solid in THF-d_8 revealed decomposition of **3** to **1** and **2**.

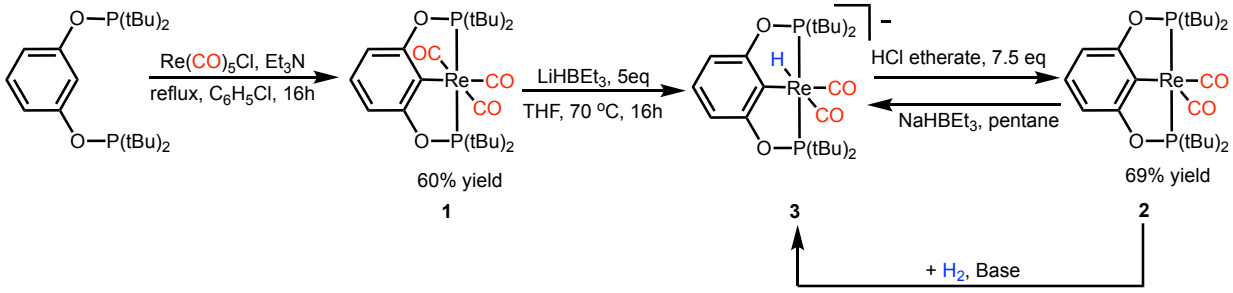

Figure 3: Synthesis of novel rhenium carbonyl pincer complexes and subsequent metal hydrides.

Measurement of hydricity in various solvents

In order to measure the hydricity of **3** in various solvents, the H_2 heterolysis method was employed. By combining **2** and a base of sufficient pK_a under an atmosphere of H_2 at 1 atm and 25 ˚C, the hydride **3** can be formed. Careful selection of the base allows for measurements of K_{eq}, ultimately enabling direct determination of the hydricity of **3** (**Scheme 1**). The hydricity of **3** was determined

in solvents relevant to catalysis (THF) as well as acetonitrile for facile comparison to the most widely utilized non-aqueous hydricity scale.[1,2,6]

Table 1: *Hydricity values in THF and MeCN, calculated based on K_{eq} of reaction and pK_a of base.* [a]*-Similar experiments were also carried out in toluene, but lack of known pK_a scale and ΔG_{H2} prevented us from determining ΔG_{H-}.* [c] *TBD = 1,5,7-Triazabicyclo[4.4.0]dec-5-ene.* [d]*DBU = 1,8-Diazabicyclo[5.4.0]undec-7-ene*

Solvent/Base[a]	**pKa**[12]	**ΔG_{H2}**[6,7] (kcal/mol)	**ΔG_{H-}** (kcal/mol)
THF; TBD[b]	20.3	68	36.75 ±1.45
MeCN; DBUc	24.34	76	40.96 ± 0.09

The newly synthesized metal hydride was found to be more hydridic than about three-fourths of reported metal hydrides in acetonitrile, but less hydridic than other anionic hydrides.[6] In addition, **3** was found to be more hydridic than formate in MeCN (ΔG = 44 kcal/mol)[6] and THF (ΔG = 42.7)[7]. This implies that **1** should preferable transfer its hydride to CO_2 to make formate ($\Delta\Delta G$ = 3.04 kcal/mol in MeCN, 5.95 kcal/mol in THF) and that this transformation would be more favorable in THF than MeCN, given its larger $\Delta\Delta G$ value. To test this, addition of 1 atm of 1:1 H_2/CO_2 blend to **2** and TBD in THF led to formation of a sharp aldehyde signal in the ^{1}H NMR spectrum at 8.43 ppm, indicative of hydride transfer to CO_2 to form formate.

Thermal equilibrium of rhenium hydride formation

While probing the metal hydride species for reactivity, solutions containing hydride **3** under H_2 in the presence of a base were found to change color as a function of temperature. At low temperatures the solution was colorless, as expected for hydride **3**, while heating the tube led to a darker brown color of dicarbonyl **2**. To understand how these temperature-dependent changes might be tied to catalysis, we investigated the speciation of **2** and **3** and the thermodynamics of H_2 splitting at variable temperatures.

Temperature dependence of hydride formation was explored using variable temperature ^{1}H NMR spectroscopy. **2** and base were added to a Teflon-sealed NMR tube and filled with one atmosphere of H_2 at room temperature.[a] After equilibration, variable temperature NMR spectroscopy was used to measure the impact of temperature on speciation. K_{eq} was determined across a variety of temperature ranges in toluene (301–375 K), THF (272–329 K), and MeCN (293–328 K).[b] At temperatures below 329 K, only **3** was observed in toluene. On the other hand, only **2** was observed in THF and MeCN above 306 K and 320 K respectively. This would suggest that hydride concentrations at elevated temperatures in THF or MeCN would approach 0 and therefore be far less active for hydrogenation catalysis. On the other hand, toluene would be less sensitive to temperature, as mild heating (< 60 ˚C) has no measurable impact on hydride concentration. Overall,

this suggests that catalytic hydrogenations using **2** may be more effective at lower temperatures due to higher concentrations of the active species, **3**.

By measuring the observed equilibrium constants (**Eq. 1**) at various temperatures, we can construct van't Hoff plots and thus deduce the ΔH and ΔS values for H_2 heterolysis. A representative plot is shown below (**Figure 4**), and constants for toluene, THF, and MeCN are reported (**Table 2**).

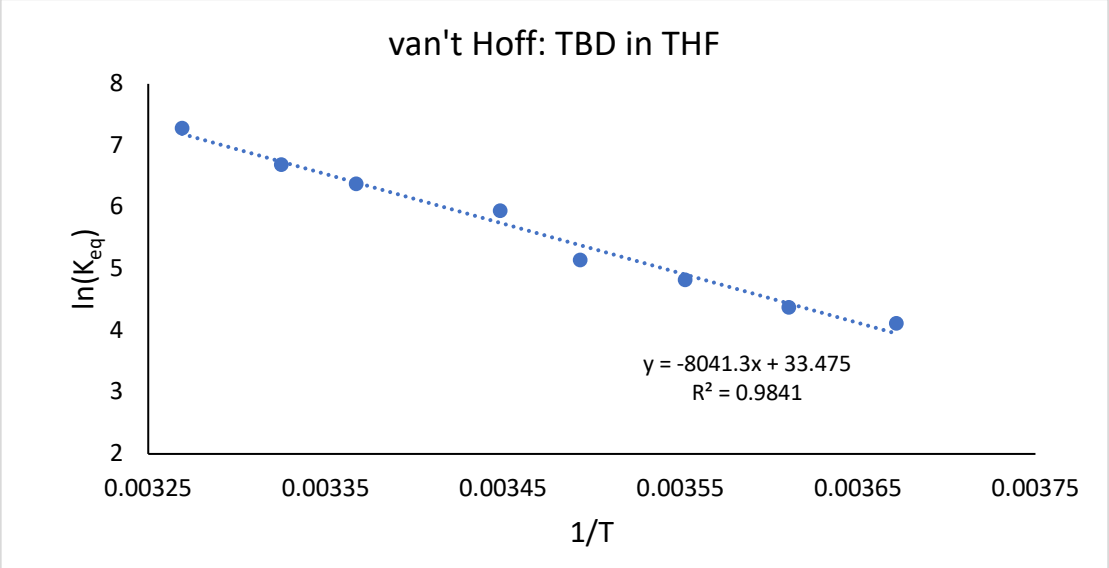

Figure 4: *van't Hoff plot constructed by calculating the equilibrium constant at various temperatures of equation* 1, *where the slope is representative of -ΔH/R and the intercept gives ΔS/R.*

Table 2: *Enthalpy, entropy, and free energy values for equation* 1 *in different solvents, averaged over 2 trials, error calculated as the standard deviation. Free energy values extrapolated to temperatures beyond the experimental range are given in parentheses (calculated using* $\Delta G^o = \Delta H^o - T\Delta S^o$*). Free energy values extrapolated to pressures outside experimental range are similarly given in parentheses (calculated by adding* $\Delta G^o_p = -1.364\log(1/\text{pressure})$ *to reported* ΔG^o *at temperature)*
[a] *Verkade's base: 2,8,9-Triisobutyl-2,5,8,9-tetraaza-1-phosphabicyclo[3.3.3]undecane*

Solvent/Base	ΔH^o (kcal/mol)	ΔS^o (cal/mol•K)	$\Delta G_{273K,\ 1atm}$ (kcal/mol)	$\Delta G_{298K,\ 1\ atm}$ (kcal/mol)	$\Delta G_{373K,\ 1\ atm}$ (kcal/mol)	$\Delta G_{298K,50\ atm}$ (kcal/mol)
Toluene; Vk's[a]	31.71 ± 0.11	91.39 ± 3.17	(6.76)	(4.48)	-2.63 ± 1.58	(5.73)
THF; TBD	15.72 ± 0.36	60.96 ± 7.85	-1.01 ± 1.73	-2.38 ± 1.97	(-7.02)	(-1.19)
MeCN; DBU	25.47 ± 2.58	93.18 ± 9.29	(0.03)	-2.31 ± 0.33	(-9.28)	(-1.05)

A recent study of a popular (PNP)Ru(CO) catalyst (PNP = 2,6-bis(di-tert-butylphosphinomethyl)pyridine) also explored the thermodynamics of H_2 heterolysis in a bimolecular system with a non-innocent pincer ligand acting as an internal base **(Figure 5)**.[13] In THF, van't Hoff analysis of (PNP)Ru(CO) revealed an enthalpy of H_2 heterolysis (ΔH° = 17.4 ± 0.2 kcal/mol) and entropy of H_2 heterolysis (ΔS° = 45 ± 0.5 cal/(mol•K)). The enthalpies in both (PNP)Ru(CO) and (POCOP)Re(CO)$_2$ are similar (within 2 kcal/mol) but the entropies observed for (POCOP)Re(CO)$_2$ are larger (by ~15 cal/(mol•K)). This large increase in entropy is likely due to the shift from a bimolecular reaction between (PNP)Ru(CO) and H_2 to a termolecular reaction with (POCOP)Re(CO)$_2$, base, and H_2.

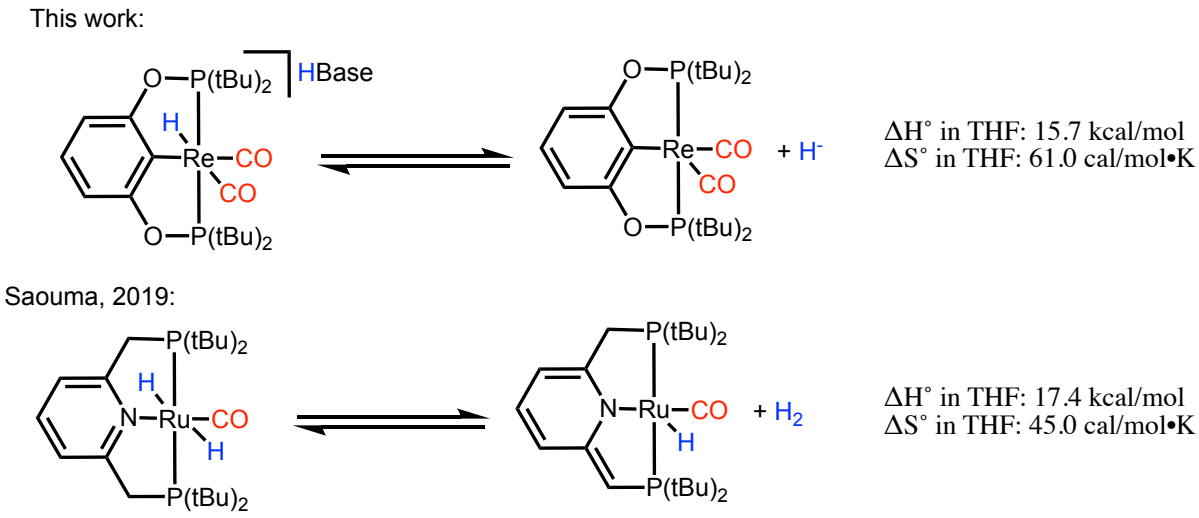

Figure 5: *Comparison of work done in this paper to a similar study using a popular (PNP)Ru(CO) catalyst.*[13]

From these data we can determine the free energy of H_2 heterolysis at a given temperature and pressure, and found that heterolysis is most favorable at low temperatures across solvents. Toluene samples were 100% **3** at room temperature and tended towards 1:1 mixtures of **2** and 3 at higher temperatures while THF and MeCN samples were 1:1 mixtures at room temperature and tended towards undetectable concentrations of **3** upon heating.

These experiments help determine the temperature at which active catalyst concentration is the greatest. In addition, the necessary pK_a of base to achieve optimal formation of metal hydride can be calculated. With this information, it should be easier to design reaction conditions for hydrogenations.

Preliminary Catalysis of CO_2 to Formate

To test the applicability of our thermodynamic results, we performed three catalytic reactions at different temperatures. **2** and 100 equivalents of TBD were added to 3 Teflon-sealed flasks with 5 mL of THF. Each was freeze-pump-thawed and allowed to equilibrate at 0 °C, 25 °C, and 50 °C

respectively. They were then filled with 1 atm of a 1:1 H_2/CO_2 gas mixture for 1.5h and left open to the gas line to ensure no pressure drop. Addition of gas led to immediate precipitation of solid. At the end of 1.5h, all vessels were frozen, the headspace was removed to stop the reaction, and solvent was subsequently removed during thawing resulting in off-white solids. The solids were dissolved in one mL of a 0.05M sodium tosylate D_2O solution and formate was quantified by NMR.

We predicted that reactions at lower temperatures would produce more formate, as there should be a larger concentration of hydride at equilibrium. However, we observed 14 TON, 43 TON, and 85 TON at 0 ºC, 25 ºC, and 50 ºC respectively. This could indicate that hydride transfer may not be the rate limiting step in this system. Other factors, such as increased base and H_2 solubility, might also influence the reaction. Further experiments must be conducted to definitively interpret these results.

Unfortunately, there are not a large number of reported hydrogenations at these milder conditions. A recent paper on a bimetallic nickel gallium system at similar reaction conditions (RT, 1 atm H_2/CO_2, THF) reported 250 TON (41 TOF) of formate with 275 equivalents of base (**Figure 6**). The system without gallium, however, only reported 0.8 TON.[14] Finding exactly comparable conditions thus far have been unfruitful.

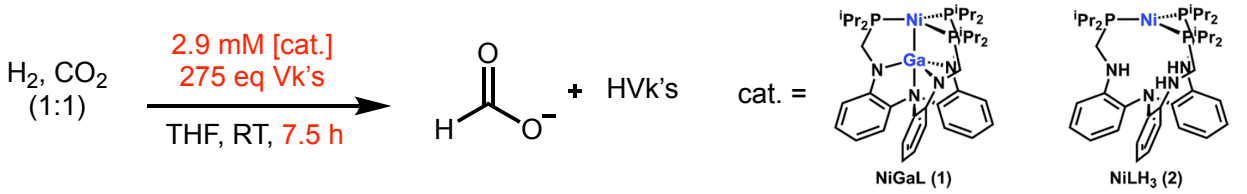

Figure 6: *Overview of leading ambient condition CO_2 hydrogenation system. Catalyst 1 reported 250 TON while 2 reported 0.8 TON.*[14]

Conclusion:

Novel rhenium complexes have been synthesized and well characterized. These include (^{tBu}POCOP)Re(CO)$_3$ **(1)** and (^{tBu}POCOP)Re(CO)$_2$ (**2**) as well as (^{tBu}POCOP)(Re)(CO)$_2$(H)$^-$. Efforts to characterize **3** have proven more difficult due to its instability to vacuum. Hydricity values for **3** at room temperature have been experimentally determined (THF: 36.75 kcal/mol; MeCN: 40.96 kcal/mol). Enthalpy and entropy values for H_2 heterolysis using **3** have also been found, and the free energy of heterolysis at different conditions have been calculated in various solvents. Preliminary hydrogenation reactions and catalytic systems have been carried out using (^{tBu}POCOP)(Re)(CO)$_2$(H)$^-$. These findings could be applied to the design of catalytic hydrogenation systems across metal complexes and guide towards more environmentally friendly reaction conditions.

Experimental:

Synthesis of (^{tBu}POCOP)(Re)(CO)$_3$ (1). In a glovebox, ^{tBu}POCOP-H (202.6 mg, 0.507 mmol) was dissolved in 5 mL of chlorobenzene and Re(CO)$_5$(Cl) (208.4 mg, 0.576 mmol) was suspended

in 5 mL of chlorobenzene. The suspensions were combined in a Schlenk flask and Et_3N (0.157 mL, 1.13 mmol) was added. After refluxing for 16h, the clear suspension turned into a pale-yellow solution. The solution was dried under vacuum without heating, leaving a sticky off-white solid. In the glovebox, the solid was extracted with pentane (2 x 5 mL) and filtered. The pale-yellow filtrate was dried, giving a light yellow microcrystalline solid. The solid was dissolved in minimal pentane and placed in the freezer overnight, resulting in precipitation of a crystalline solid. The mother liquor was decanted, the volume was reduced by half, and placed back in the freezer for a second recrystallization. The resulting crystals were dried yielding 204.0 mg of pale-yellow crystals (60% yield). The material was found to be >99% pure by multinuclear NMR spectroscopy. NMR and elemental analysis are reported for the isolated crystals. Single crystal x-ray diffraction studies were run on crystals isolated from the mother liquor. **^{1}H NMR** (600 MHz, d_8-benzene): δ 6.93 (t, 7.9 Hz, 1H), 6.80 (d, 7.8 Hz, 2H), 1.29 (m, 36H). **^{31}P{^{1}H} NMR** (162 MHz, d_8-benzene): δ 188.94 (s). **^{13}C{^{1}H}** (151 MHz, d_8-benzene): δ 200.83 (t, 8.8 Hz), 200.14 (s), 167.41 (t, 6.5 Hz), 130.77 (t, 7.3 Hz), 127.65 (s), 105.71 (t, 4.8 Hz), 43.03 (t, 10.4 Hz), 29.33 (t, 2.9). **IR** 1902 cm^{-1}, 1923 cm^{-1}, 2023 cm^{-1}. **Anal. Calcd** for $C_{25}H_{39}O_5P_2Re$: C, 44.97; H, 5.89; N, 0.00. Found: C, 45.06; H, 5.72; N, <0.02.

Synthesis of (^{tBu}POCOP)(Re)(CO)$_2$ (2). In a glovebox, **1** (49.5 mg, 0.074 mmol) was dissolved in 5 mL of THF and lithium triethylborohydride (371 µL of a 1M solution in THF, 0.371 mmol) was added by syringe. The solution was transferred to a Teflon sealed pressure vessel and heated at 70 °C overnight. The excess CO was then removed through five freeze-pump-thaw cycles. In the glovebox, the clear solution was stirred while adding HCl (290 µL of a 2M solution in diethyl ether, 0.580 mmol). The solution immediately turned dark brown. After stirring for 10 minutes, the solution was dried under vacuum. The product was extracted with pentane (3 x 2 mL), filtered, and dried under vacuum, yielding 32.6 mg of a dark brown solid (69% yield). The material was found to be >99% by multinuclear NMR spectroscopy and elemental analysis. NMR and elemental analysis are reported for the isolated powder. Single crystal x-ray diffraction data was collected on crystals grown via slow evaporation of a pentane solution. **^{1}H NMR** (600 MHz, d_8-benzene): δ 7.13 (t, 7.9 Hz, 1H), 6.88 (d, 7.9 Hz, 2H), 1.21 (m, 36H). **^{31}P{^{1}H} NMR** (243 MHz, d_8-benzene): δ 210.76 (s). **^{13}C{^{1}H}** (151 MHz, d_8-benzene): δ 206.21 (t, 4.0 Hz) 167.29 (t, 8.6 Hz), 161.54 (t, 7.6 Hz), 129.49 (s), 99.69 (t, 5.1 Hz), 36.55 (t, 10.2 Hz), 22.90 (br s). **IR** 1834 cm^{-1}, 1911 cm^{-1}. **Anal. Calcd** for $C_{24}H_{39}O_4P_2Re$: C, 45.06; H, 6.15; N, 0.00. Found: C, 45.34; H, 6.11; N, <0.10.

Synthesis of [Na][(^{tBu}POCOP)(Re)(CO)$_2$(H)] (3). In a glovebox, **2** (20 mg, 0.031 mmol) was dissolved in 5 mL toluene. Sodium triethylborohydride (34.5 µL of a 1M solution in toluene, 0.0345 mmol) was added followed by 10 mL of pentane and allowed to sit for 16 h, during which a white precipitate forms and the solution turns from dark brown to yellow. The solution was decanted and washed with toluene (3 x 2 mL), then dried for one minute. The material was found to be 93% pure by multinuclear NMR spectroscopy (the other 7% was found to be **2**). **^{1}H NMR** (400 MHz, d_8-THF): δ 6.41 (t, 7.6 Hz, 1H), δ 6.20 (d, 7.7 Hz, 2H), δ 1.44 (m, 18H), δ 1.33 (m,

18H), δ -6.10 (t, 25.77 Hz, 1H). **$^{31}P\{^{1}H\}$ NMR** (161.92 MHz, d_8-THF): δ 201.68 (s). **IR** 1873 cm^{-1}, 1754 cm^{-1}, 1737 cm^{-1}.

Preparation of samples for hydricity measurements. In a glovebox, **2** (5 mg, 0.008 mmol) and one equivalent of base were dissolved in 0.5 mL deuterated solvent in a Teflon sealed NMR tube. Ten µl of a mesitylene stock solution (2.5 µl in 197.5 µl solvent) was injected. The tube was then freeze-pump-thawed three times to remove atmosphere and backfilled with 1 atm of H_2 gas at 298 K. The sample was monitored my ^{1}H NMR spectroscopy every 24h until equilibrium was reached.

Process of thermal hydricity measurements. Samples from above were placed in a Neo400 spectrometer. The probe temperature was then raised by 10 °C and the sample was allowed to equilibrate for 4 minutes before each spectrum was collected. This process was repeated until the boiling point of the solvent was approached. The probe temperature was then reduced by 5 °C and allowed to equilibrate for 4 minutes before a spectrum was collected. Data was collected again in intervals of 10 °C decreasing until the lower limit was reached. van't Hoff plots were constructed by plotting the inverse of temperature against $\ln(K_{eq})$.

References:

(1) Dub, P. A.; Ikariya, T. Catalytic Reductive Transformations of Carboxylic and Carbonic Acid Derivatives Using Molecular Hydrogen. *ACS Catal.* **2012**, *2* (8), 1718–1741. https://doi.org/10.1021/cs300341g.

(2) Werkmeister, S.; Junge, K.; Beller, M. Catalytic Hydrogenation of Carboxylic Acid Esters, Amides, and Nitriles with Homogeneous Catalysts. *Org. Process Res. Dev.* **2014**, *18* (2), 289–302. https://doi.org/10.1021/op4003278.

(3) Hankin, A.; Shah, N. Process Exploration and Assessment for the Production of Methanol and Dimethyl Ether from Carbon Dioxide and Water. *Sustain. Energy Fuels* **2017**, *1* (7), 1541–1556. https://doi.org/10.1039/c7se00206h.

(4) Rezayee, N. M.; Huff, C. A.; Sanford, M. S. Tandem Amine and Ruthenium-Catalyzed Hydrogenation of CO2to Methanol. *J. Am. Chem. Soc.* **2015**, *137* (3), 1028–1031. https://doi.org/10.1021/ja511329m.

(5) Gribble, G. W. Sodium Borohydride in Carboxylic Acid Media: A Phenomenal Reduction System. *Chem. Soc. Rev.* **1998**, *27* (6), 395–404.

(6) Wiedner, E. S.; Chambers, M. B.; Pitman, C. L.; Bullock, R. M.; Miller, A. J. M.; Appel, A. M. Thermodynamic Hydricity of Transition Metal Hydrides. *Chem. Rev.* **2016**, *116* (15), 8655–8692. https://doi.org/10.1021/acs.chemrev.6b00168.

(7) Brereton, K. R.; Jadrich, C. N.; Stratakes, B. M.; Miller, A. J. M. Thermodynamic Hydricity across Solvents: Subtle Electronic Effects and Striking Ligation Effects in Iridium Hydrides. *Organometallics* **2019**, *38* (16), 3104–3110. https://doi.org/10.1021/acs.organomet.9b00278.

(8) Vogt, M.; Nerush, A.; Diskin-Posner, Y.; Ben-David, Y.; Milstein, D. Reversible CO2 Binding Triggered by Metal-Ligand Cooperation in a Rhenium(i) PNP Pincer-Type Complex and the Reaction with Dihydrogen. *Chem. Sci.* **2014**, *5* (5), 2043–2051. https://doi.org/10.1039/c4sc00130c.

(9) Piehl, P.; Peña-López, M.; Frey, A.; Neumann, H.; Beller, M. Hydrogen Autotransfer and Related Dehydrogenative Coupling Reactions Using a Rhenium(i) Pincer Catalyst. *Chem. Commun.* **2017**, *53* (22), 3265–3268. https://doi.org/10.1039/c6cc09977g.
(10) Kosanovich, A. J.; Reibenspies, J. H.; Ozerov, O. V. Complexes of High-Valent Rhenium Supported by the PCP Pincer. *Organometallics* **2016**, *35* (4), 513–519. https://doi.org/10.1021/acs.organomet.5b00935.
(11) Vogt, M.; Nerush, A.; Iron, M. A.; Leitus, G.; Diskin-Posner, Y.; Shimon, L. J. W.; Ben-David, Y.; Milstein, D. Activation of Nitriles by Metal Ligand Cooperation. Reversible Formation of Ketimido- and Enamido-Rhenium PNP Pincer Complexes and Relevance to Catalytic Design. *J. Am. Chem. Soc.* **2013**, *135* (45), 17004–17018. https://doi.org/10.1021/ja4071859.
(12) Kaljurand, I.; Kütt, A.; Sooväli, L.; Rodima, T.; Mäemets, V.; Leito, I.; Koppel, I. A. Extension of the Self-Consistent Spectrophotometric Basicity Scale in Acetonitrile to a Full Span of 28 PKa Units: Unification of Different Basicity Scales. *J. Org. Chem.* **2005**, *70* (3), 1019–1028. https://doi.org/10.1021/jo048252w.
(13) Mathis, C. L.; Geary, J.; Ardon, Y.; Reese, M. S.; Philliber, M. A.; Vanderlinden, R. T.; Saouma, C. T. Thermodynamic Analysis of Metal-Ligand Cooperativity of PNP Ru Complexes: Implications for CO2 Hydrogenation to Methanol and Catalyst Inhibition. *J. Am. Chem. Soc.* **2019**, *141* (36), 14317–14328. https://doi.org/10.1021/jacs.9b06760.
(14) Cammarota, R. C.; Vollmer, M. V.; Xie, J.; Ye, J.; Linehan, J. C.; Burgess, S. A.; Appel, A. M.; Gagliardi, L.; Lu, C. C. A Bimetallic Nickel-Gallium Complex Catalyzes CO2 Hydrogenation via the Intermediacy of an Anionic D10 Nickel Hydride. *J. Am. Chem. Soc.* **2017**, *139* (40), 14244–14250. https://doi.org/10.1021/jacs.7b07911.